Title:

Wildfire air pollution hazard during the 21st century

Authors:

Wolfgang Knorr*[1,2], Frank Dentener[3] , Jean-François Lamarque[4], Leiwen Jiang[4,5] & A. Arneth[2]

[1]Physical Geography and Ecosystem Analysis, Lund University, Sölvegatan 12, 22362 Lund, Sweden

[2]KIT/IMK-IFU, Garmisch-Partenkirchen, Germany

[3]European Commission, Joint Research Centre, Ispra, Italy.

[4]National Center for Atmospheric Research, Boulder, Colorado, USA

[5]Asian Demographic Research Institute, Shanghai University

*Corresponding author's email: wolfgang.knorr@nateko.lu.se

Abstract:

Wildfires pose a significant risk to human livelihoods and are a substantial health hazard due to emissions of toxic smoke. Previous studies have shown that climate change, increasing atmospheric CO_2, as well as human demographic dynamics can lead to substantially altered wildfire risk in the future, with fire activity increasing in some regions and decreasing in others. The present study re-examines these results from the perspective of air pollution risk, focussing on emissions of airborne particulate matter ($PM_{2.5}$), combining an existing ensemble of simulations using a coupled fire–dynamic vegetation model with current observation-based estimates of wildfire emissions and simulations with a chemical transport model. Currently, wildfire $PM_{2.5}$ emissions exceed those from anthropogenic sources in large parts of the world. We further analyse two extreme sets of future wildfire emissions in a

socio-economic, demographic climate change context, and compare them to anthropogenic emission scenarios reflecting current and ambitious air pollution legislation. In most regions of the world, ambitious reductions of anthropogenic air pollutant emission have the potential to limit mean annual pollutant $PM_{2.5}$ levels to comply with WHO air quality guidelines for $PM_{2.5}$. Worse-case future wildfire emissions are not likely to interfere with these annual goals, largely due to fire seasonality, as well as a tendency of wildfire sources to be situated in areas of intermediate population density, as opposed to anthropogenic sources that tend to by highest at the highest population densities. However, during the high-fire season, we find many regions where future $PM_{2.5}$ pollution levels can reach dangerous levels even for a scenario of aggressive reduction of anthropogenic emissions.

1 Introduction

Wildland fires – or in short "wildfires" – are burning events that occur in natural or semi-natural landscapes such as (managed or un-managed) forests, shrublands, or grazing lands including savannahs. They are a major natural hazard (Bowman et al. 2009) and an important source of air pollutants (Langmann 2009), which can impact air pollution thousands of kilometres downwind (Lee et al. 2005). Wildfires also play an important role in several atmospheric chemistry–climate feedback mechanisms (Fiore et al. 2012). Emissions of fine aerosol particles, i.e. particulate matter up to an aerodynamic diameter of 2.5 micrometers ($PM_{2.5}$), are of particular health concern, with no known safe concentration in air, as noted by the World Health Organization (WHO 2006). Wildfires can be an important source in large, more remote areas (Granier et al. 2011, van der Werf et al. 2010), even though anthropogenic emissions are higher globally. There is a widely held view among both the general public and members of the research community that wildfire occurrence and severity have been

increasing in recent decades, and will continue to increase due to climate change (Doerr and Santin 2016). Moreover, efforts to reduce anthropogenic emissions (e.g. EEA 2014) will increase the relative importance of other emission sources.

Climate warming has already led to more frequent hot and dry weather in many parts of the globe, increasing the probability of wildfires (Flannigan et al. 2009), and this is expected to continue into the future. Studies based on calculated fire severity indices under climate change argue for large increases in burned area (Flannigan et al. 2005 for Canada; Amatulli et al. 2013 for southern Europe) and resultant pollutant emissions (Spracklen et al. 2009, Yue et al. 2013 for the western US), with some regional exceptions of declining emissions due to increased precipitation (Yue et al. 2015 for a few sub-regions in northern Canada). However, a long-term increase in the length of the fire season or in weather conditions conducive of wildfires does not necessarily lead to increases in burned area (Doerr and Santin 2016). This is because, at longer time scales, vegetation responds not only to climate change, but also directly to rising atmospheric CO_2 levels (Buitenwerf et al. 2012, Donohue et al. 2013). While CO_2 fertilization will lead to increased fuel load, enhancing emissions, it also leads to an increase in woody as opposed to herbaceous vegetation, with on average lower emissions due to decreased fire spread in less flammable shrublands (Kelley and Harrison 2014, Knorr et al. 2016a). Indeed, simulations with coupled fire-vegetation or statistical models generally show less increase in burned area (Kloster et al. 2010, Knorr et al. 2016b) or number of fires (Krwachuk et al. 2009) when accounting not only for climate, but also for these vegetation effects.

Another factor that has so far received less attention are growth and changes in human population size and distribution. Contrary to common perception, higher population density tends to be associated with lower wildfire risks when measured by

burned area (Archibald et al. 2009, 2010, Lehsten et al. 2010, Knorr et al. 2014, Bistinas et al. 2014), even though higher population density in rural and remote regions tends to lead to more, but on average smaller fires (Archibald et al. 2009, 2010). This can be explained by the concept of the ignition-saturated fire regime, which is reached at very low levels of population density. Above this level, human impact manifests itself less in enhancing burned area (by igniting fires), but more by creating barriers to and suppressing fire spread, thus reducing area burned (Guyette et al. 2002). Indeed, coupled vegetation–fire models that include the effects of changing human population size and spatial distribution suggest a reduced rate of increase of fire activity during the 21st century, compared to simulations not accounting for demographic changes (Kloster et al. 2010). Some studies showed even a decline in burned area (Knorr et al. 2016b) or emissions (Knorr et al. 2016a) for moderate levels of climate change, when combined with slow urbanisation and high population growth. These results are backed by observational evidence of a long-term declining trend in past fire activity or emissions from wildfires (Marlon et al. 2008, Wang et al. 2010, van der Werf et al. 2013), and more recent negative trends in northern Africa that have been related to the expansion of cropland (also resulting from increasing population density; Andela and van der Werf 2014). Furthermore, the impacts of emissions from wildfires on human society are also largely determined by population growth and their spatial distribution (Knorr et al. 2016 b). It is therefore important to consider not only climate and CO_2 scenarios, but also scenarios of demographic changes.

The overarching research question addressed in this paper is whether socio-economic developments influencing both greenhouse gas emissions as well as human population size and spatial distribution might impact wildfire emissions enough to make a difference for meeting the WHO air quality target, provided anthropogenic $PM_{2.5}$ emissions are reduced aggressively. The work in this

study takes the following steps towards this end: Building on a similar study for Europe (Knorr et al. 2016 c) for computing emissions, we use a state-of-the art chemical transport model to compute future levels of human exposure to $PM_{2.5}$ using observation-based wildfire emissions, combined with relative changes in emissions from vegetation–fire model simulations. Our analysis focuses on the relative importance of changes in global wildfire emissions for air quality and atmospheric pollutant load, as compared to anthropogenic sources.

2 Methods

2.1 Vegetation–fire model and driving data

We use the LPJ-GUESS global dynamic vegetation model (Smith et al. 2001, Ahlström et al. 2012) coupled to the global semi-empirical fire model SIMFIRE (Knorr et al. 2014), with details given by Knorr et al. (2016a). Shortly, LPJ-GUESS is a patch-scale dynamic vegetation model that represents age cohorts of perennial vegetation and computes vegetation establishment and growth, allocation of carbon pools in living plants, and turnover of carbon in plant litter and soils. SIMFIRE provides burned area to LPJ-GUESS on an annual basis, which then evokes plant mortality according to a plant-functional-type (PFT) dependent probability. Specified fractions of plant litter and live leaf biomass are burnt and emitted into the air in a fire, while the remaining biomass of the killed vegetation is transferred to the litter pool of LPJ-GUESS (see Knorr et al. 2012). Population data needed to drive SIMFIRE are based on gridded data from HYDE 3.1 (Klein-Goldewijk et al. 2010) up to 2005, and then re-scaled using per-country relative growth in rural and urban population, retaining the urban masks of the HYDE data. Grid cells with more than 50% past or future cropland area in either the RCP6.0 or 4.5 land use scenarios (Hurtt

et al. 2011; see Section 2.2) were excluded from the calculations (see Knorr et al. 2016a,b for details).

In order to compute emissions of chemical species, we use the emission factors of the Global Fire Emissions Database version 4 (GFED 4, van der Werf et al. 2010, based mainly on Akagi et al. 2011, see http://www.falw.vu/~gwerf/GFED/GFED4), which are fixed ratios between emission rates of various pollutant species and rates of combustion of dry biomass differentiated by where the fire occurs: (1) savannahs and grasslands, (2) tropical, (3) boreal and (4) temperate forests. In order to select the appropriate emissions factor, we assign a grid cell to (1) if the PFT with the largest leaf area index at full leaf development is a grass, to (2) if it is a tropical tree, and to (3) or (4) if it is a boreal or temperate tree, respectively (see Knorr et al. 2012 for a list of PFTs used).

2.2 Simulations and scenarios

Climate simulations were driven by output from an ensemble of eight global climate models from the Climate Model Intercomparison Project 5 (CMIP5, Taylor et al. 2012) for two climate scenarios based on the Representative Concentration Pathways (van Vuuren et al. 2011) RCP4.5 with moderate, and RCP8.5 with high degree of climate change. Simulations for 1901 to 2100 are carried out on a global equal-area grid with 1° x 1° spatial resolution at the equator, but constant east-west spacing of the grid cells when moving towards the poles in order to keep the grid cell area constant (Knorr et al. 2016a). These climate scenarios were combined with population and urbanisation projections following the Shared Socioeconomic Pathways (SSPs, Jiang 2014). The SSPs are based on qualitative narratives of five different development pathways, which have been translated into quantitative projections of a range of socio-economic, demographic and biophysical factors. Here, we focus on

two combinations that represent, respectively, the highest and lowest wildfire combusted carbon emissions globally (Knorr et al. 2016a). These are RCP8.5 (high greenhouse-gas emissions, strong warming) combined with SSP5 (rapid fossil-fuel driven economic growth with globally low population growth and fast urbanisation leading to land abandonment and increased wildfire activity), and RCP4.5 (moderate greenhouse-gas emissions and climate warming) combined with SSP3 (globally high population growth and slow urbanisation leading to increased fire suppression). Note, however, that in contrast to developing countries and the world as a whole, high-income countries have high population growth for SSP5, but low population growth for SSP3.

In addition to the emissions simulated by LPJ-GUESS-SIMFIRE, we also use the GFED4.1s observation-based emissions fields for wildfires (van der Werf et al. 2010, updated using Randerson et al. 2012 and Giglio et al. 2013) aggregated to 0.5° x0.5° resolution and then re-scaled in time by country or region (following the methodology of Knorr et al. 2016c). For larger countries, scaling is done by sub-national regions, which were chosen in such a way as to isolate major fire areas found in GFED4.1s. (For a list of regions/countries, see Table S1 in the Supplementary Information). The use of country boundaries and performing the analysis at 0.5x0.5° instead of the 1°-resolution used by LPJ-GUESS-SIMFIRE better accounts for the high degree of fire-policy or cultural impact on fire regimes (Bowman et al. 2009).

For wildfires, we use the sum of boreal forest fires, temperate forest fires and savannah fires from GFED4.1s. Agricultural waste burning from GFED4.1s has been excluded from the calculations. Instead, we use anthropogenic emissions that include agricultural burning from the ECLIPSE data set (Granier et al. 2011). Deforestation fires (caused by deforestation activities) and peat fires (fires occurring in forested or

non-forested peatlands, see van der Werf et al. 2010) were found to be minor sources globally, despite of their regional importance mainly in Southeast-Asia (Fig. S1, Table S2)

In contrast to Knorr et al. (2016c), where changes in the spatial distribution of population within a country did not affect predicted wildfire emissions, here we also account for demographic effects at the grid-cell scale. To do so, we combine a scalar accounting for climate and vegetation effects, f_{cv}, which is uniform in space across each region/country, with a scalar accounting for population effects, f_p, which is applied at each grid cell separately:

$$E^S(x,y,m) = f^S_{cv}(R(x),y) * f_p(\Delta p'(x,y)) * E^S_{GFED}(x,m) \qquad (1)$$

with E^S the re-scaled per-grid-cell emissions of chemical species S, x the geographic location on the 0.5°x0.5° grid used for the analysis, y year, m month of the year, $R(x)$ the country or region found at location x, and E^S_{GFED} the (per-grid-cell) emissions climatology of species S from GFED 4.1s averaged over 1997 to 2014. The population effect, f_p , is equal to the population multiplier of SIMFIRE (Knorr et al. 2016a):

$$f_p(\Delta p') = \exp(-0.0168*\Delta p'). \qquad (2)$$

with $\Delta p'(x,y)=p'(p(x,y))-p'(p(x,y_0))$, where $p'(p)$ is the minimum of population density p and 100 inhabitants per km^2. y_0=2010 is the reference year relative to which future emission levels are computed. The cap at 100 / km^2, which is only used for scaling observation-based inventories by LPJ-GUESS-SIMFIRE output (not by SIMFIRE itself) is used to prevent unrealistically large relative increases in emissions resulting from the scaling procedure when population density decreases from present values that are much above 100 / km^2. In other words, we consider areas with a population density above 100 / km^2 to be essentially wildfire free. The combined

effect of climate and vegetation on emissions is defined as:

$$f^{S}_{cv}(R,y) = \{\Sigma_{x'\in R}\, E^{S}_{SIM}(x',y) / \Sigma_{x'\in R}\, E^{S}_{SIM}(x',y_0)\} / \ldots$$

$$\ldots \{\Sigma_{x'\in R}\, f_p(p(x',y)-p(x',y_0))E^{S}_{\mathrm{GFED}}(x',m) / \Sigma_{x'\in R}\, E^{S}_{\mathrm{GFED}}(x',m)\}. \quad (3)$$

Here, E^{S}_{SIM} are LPJ-GUESS-SIMFIRE emissions of species *S* computed on the 1° equal-area grid. The sums are over all grid cells *x'* of the 1° equal-area grid that belong to region/country *R*. The first term in curly brackets is the SIMFIRE simulated relative change in emissions or region *R* by year *y* (shown in Fig. S2), which is divided by the projected change in emissions only due to changes in population density (second term in curly brackets; see Fig. S3 for a map of projected changes only due to population density, i.e. $f_p(p'(x,y)-p'(x,y_0))$ for y=2090). Finally, we compute future projected emissions of species *S* as the 21-year climatological mean around 2090:

$$E^{S}_{2090}(x,m) = \Sigma_{y\in[2080,\,2100]}\, E^{S}(x,y,m) \quad (4)$$

Countries where 90% or more of the grid cells of the LPJ-GUESS grid have either a current or future cropland fraction of ≥50% (highly agricultural regions: Moldavia and Bangladesh), or for which LPJ-GUESS simulates zero current emissions in at least one simulation (Greenland) were excluded from this scaling procedure by setting $f^{S}_{cv}(R,y)=f_p(p)=1$. Note that the procedure retains the seasonal cycle of the GFED4.1 emissions, $E_{\mathrm{GFED}}(m)$, by scaling each month by the same factor.

The computed seasonal cycle of anthropogenic emissions of CO, NH_3, SO_2, NO_x, black carbon and organic carbon (at monthly resolution) for current conditions and 2090 were provided as input to the Community Atmosphere Model including interactive chemistry (CAM-Chem, Lamarque et al. 2012). In the present configuration, CAM-Chem simulates the aerosol distributions for all types (i.e., sulfate, nitrate, black carbon, organic carbon, sea-salt and mineral dust). From those,

the $PM_{2.5}$ distribution is calculated using all components except dust or sea-salt, since those are not affected by biomass burning, and assuming all component mass to be present below 2.5 μm. For current emissions we take $E^S_{GFED}(x,m)$, and for 2090 emissions $E^S_{2090}(x,m)$ (Eq. 4). Anthropogenic emissions are constant over the year.

The configuration of CAM-Chem is identical to the one used in the recent Chemistry-Climate Model Initiative simulations discussed in Tilmes et al. (2016) under REF-C1 (specified sea-surface temperatures and sea-ice distribution), except for using a higher horizontal resolution of 0.9° latitude x 1.25° longitude. The model has 26 vertical layers from the surface to approximately 40 km. CAM-Chem is here used as a chemical transport model, with the meteorology being the same between simulations with different emissions fields, thus excluding the effect of changing atmospheric composition on meteorology. This is done so that short simulations are sufficient to identify the chemical impacts of different emission scenarios. Emissions of sea-salt, dust and biogenic volatile organic compounds (VOCs, i.e. isoprene and mono-terpenes, which are precursors to secondary-organic aerosols) are also identical between the different simulations, and are computed as in (Tilmes et al. 2016). For all species, emissions (including biomass burning) are included as flux boundary conditions to the vertical diffusion module, and are therefore quickly (within hours) redistributed within the boundary layer.

The current representation of aerosols in CAM-Chem has been extensively tested and compared with observations. In particular, Lamarque et al. (2012) provide a comparison of present-day observations of the IMPROVE network over the conterminous United States, indicating an overall good representation of the probability density function for all species considered in the present study. In addition, Shindell et al. (2013) have shown that CAM-Chem indicated the lowest bias

of the models when compared to observed aerosol optical depth. Finally, CAM-Chem results have been used in several health impacts studies (West et al., 2013; Silva et al., 2013, 2016) and is usually very consistent with other chemistry-climate models used for those analyses. Four simulations are carried out for a period of 25 months each, and a mean annual cycle is computed from months 2 to 25. While there is some residual interannual variability in the two meteorological years simulated by the model, this signal is small compared to the impact associated with the changes in emissions (not shown).

2.3 Analytical Framework

Our analysis focuses on two time windows, current and 2090. To assess the relevance of wildfire $PM_{2.5}$ emission rates, we compare them to those from anthropogenic sources, and also judge simulated surface concentrations by their proximity to the World Health Organization (WHO) air quality guidelines of 10 $\mu g/m^3$ on an annual average, keeping in mind that there is no established safe upper limit and that the target was set considering background concentrations of 3–5 $\mu g\ m^{-3}$ in North America and Western Europe.

For anthropogenic emissions, we use the ECLIPSE-GAINS-v4a data (Amann et al., 2011) developed as part of the ECLIPSE project (Granier et al. 2011, Klimont et al. 2013, Stohl et al., 2015). This dataset provides two scenarios: current legislation (CLE), and maximum feasible reductions (MFR) on top of business-as-usual projections until 2050 from the Energy Technology Projections study by the International Energy Agency (IEA, 2012), which are considered roughly equivalent to RCP6.0. MFR corresponds to a policy and technology driven abatement scenario, implementing all currently known technologies at a reasonable cost, with the aim, among others, to lower $PM_{2.5}$ emissions to levels of limited health impacts (Amann et

al. 2011). For the present, we use emissions for 2010 under the CLE scenario. Following Knorr et al. (2016c), we estimate 2090 CLE emissions assuming constant *per capita* emissions after 2050, but changing population densities according to the SSP3 scenario, which directly affects magnitude and spatial patterns of emissions. For MFR, 2090 emissions are assumed half of the corresponding 2050 levels (i.e. somewhat optimistic compared with e.g. Braspenning-Radu et al., 2016). In principle the emissions under CLE and MFR conditions may differ also for different SSP and climate mitigation assumptions (Rao et al., 2016; Braspenning-Radu et al, 2016). However, the assumptions above can be seen as a schematic approximation of a wide range of possible air pollution emission futures that have become available in the recent literature

To facilitate the regional aspects of our analysis, we use a global map of nine major world regions (see Fig. S4). Of these, three belong to the high-income group of countries of the SSP scenarios (see Jiang and O'Neill 2015): High-income Europe, Australia & New Zealand, and North America. Countries of Europe belonging to the middle-incoming group were assigned to the region Eastern Europe and Central Asia, which also includes Russia. High-income countries of the Middle East (Israel, oil-rich states of the Persian Gulf) or East Asia (Japan, South Korea), which only account for a very small fraction of wildfire emissions in their respective regions, have been excluded from the analysis.

In this study, we address the question whether there is a risk that the combined direct (as estimated by changing population patterns) and indirect impacts (through climate change) of human activities on wildfire pollutant emissions will compromise meeting the WHO guideline value of 10 $\mu g / m^3$, under a scenario in which anthropogenic $PM_{2.5}$ emissions are reduced aggressively. The range of plausible

301 future air quality policy scenarios is spanned by the difference between our
302 projections using MFR and CLE assumptions. For a range of plausible wildfire
303 emissions scenarios, we consider the combinations SSP5/RCP8.5 (highest) and
304 SSP3/RCP4.5 (lowest global wildfire emissions). Of the possible four emission
305 combinations, we select three in order to assess the impact of either the plausible
306 range of wildfire, or of air quality policy scenarios (see Table 1). These three
307 scenarios plus current emission fields are used for simulating present and future
308 (2090) $PM_{2.5}$ surface concentrations with CAM-Chem.

309 # 3 Results

310 ## *3.1 Comparison of wildfire and anthropogenic pollutant emissions*

311 In order for wildfire emissions to be relevant for atmospheric pollution levels, at
312 least two conditions should be met: (1) they need to be of a similar or greater
313 magnitude compared to anthropogenic sources, and (2) they should be in or close to
314 populated areas. Therefore we first compare emission levels of both types of sources
315 for the current and future time slices. Fig. 1 shows areas where wildfire emissions
316 currently exceed those from anthropogenic sources (in either red or light blue; shown
317 in all panels). At first sight, these regions appear to lie in relatively remote areas of
318 wildfire-prone regions (cf. Fig. S5, e.g. the boreal forest zones of Canada and Alaska,
319 eastern Siberia, western US, the Brazilian interior, and in Africa away from the main
320 population centres of Nigeria, Ethiopia and Kenya). A breakdown of emissions by
321 population density shown for the nine world regions (cf. Fig. S4) shows that current
322 (or future) anthropogenic emissions display a universal increase with increasing
323 population density (solid blue lines in Fig. 2). Wildfire emissions also often increase
324 with increasing population density, and only for North America per-area emissions
325 decrease with increasing population density across the entire range of population

densities (dashed blue lines in Fig. 2, i.e. current wildfire emissions). Most of the remaining regions have peaked distributions with highest per-area emissions in some intermediate population-density category, and it is not the most remote and sparsely inhabitated areas that have the highest emissions. Therefore, despite of a dominance of anthropogenic emissions in the more densely populated areas, wildfires emissions are often found to be an important pollution source in regions with intermediate population density, meaning that they approach or even exceed anthropogenic sources for population densities in the range 10 to 100 / km^2 (Sub-Saharan Africa, Latin America & Caribbean, South & Southeast Asia, Australia & New Zealand). This 10 to 100 / km^2 category is significant not only because of its relatively high population density, but also because it represents the wildland-urban interface, which is often particularly prone to wildfires (Syphard et al. 2007).

For the simulated future, we either expect anthropogenic emissions to surpass those from wildfires in many regions (mainly in Africa, light blue areas in Fig. 1a, b) for the CLE scenario, or the reverse for the MFR scenario, where wildfire emissions surpass anthropogenic sources in a wide range of regions (yellow areas in Fig. 1c, d: South America, Central America, Africa, Eastern and Southern Europe, Central Asia, Southeast Asia, and southern China). This dominant role of the anthropogenic-emissions scenario is largely independent of the wildfire emissions scenario (i.e. the difference between Fig. 1a and b or between Fig. 1b and d is much small than the difference between Fig. 1a, b on the one hand and Fig. 1 c, d on the other). The strongest impact of the wildfire emissions scenario is found for Sub-Saharan Africa for the CLE scenario, where SSP3/RCP4.5 shows many more regions newly dominated by anthropogenic emissions than SSP5/RCP8.5 (Fig. 1a vs. Fig. 1b). This is due to declining wildfire emissions in that scenario (see Fig. S2a). The scenario in

351 which wildfire emissions are most likely to become a relevant source of $PM_{2.5}$
352 emissions is represented by the combination MFR/SSP5/RCP8.5 (Fig. 1d and Fig. 2,
353 red lines; cf. also Fig. S2b).

354 The MFR scenario assumes a decline in anthropogenic emissions by
355 approximately one order of magnitude in areas with at least 10 people / km^2, with
356 somewhat less decrease for the more sparsely populated categories (Fig. 2). When
357 compared to this magnitude of change, the simulated increase in wildfire emissions
358 for SSP5/RC8.5 is much smaller throughout. The highest absolute increase for
359 wildfire emissions is found for Sub-Saharan Africa (in the 1 to 100 / km^2 categories),
360 Latin America (0.1 to 1 / km^2), South & Southeast Asia (below 10 / km^2) and
361 Developing East Asia (1 to 100 / km^2). As a consequence mainly of the reduction
362 implicit in the MFR scenario, wildfire emissions approach or exceed anthropogenic
363 emissions even in the most densely populated category (>100 / km^2) for Sub-Saharan
364 Africa, Latin America & Caribbean, Eastern Europe-Russia-Central Asia, South &
365 Southeast Asia and Australia & New Zealand. Note that the areas of the population
366 density categories shift as well (see dotted lines in Fig. 2 and Fig. S5), and that the
367 underlying population patterns used to compute the MFR scenario do not necessarily
368 match those from SSP5.

369 ***3.3 Changing patterns of $PM_{2.5}$ pollutant exposure***

370 Simulated changes of $PM_{2.5}$ concentrations between current and 2090 for the high-
371 wildfire emissions scenario combined with MFR (Fig. 3 blue to red line,
372 corresponding to emissions of Fig. 2, same colours) indicate a reduction in $PM_{2,5}$
373 pollutant concentration by between one half and three-quarters in the most densely
374 populated category (>100 / km^2) in each world region, resulting from the large

reductions in anthropogenic emissions. Both the current and future pollution levels are substantially lower in the most sparsely populated categories. For current emissions, only two regions show average anthropogenic concentrations above the WHO air-quality target of 10 μg / m^3 (Developing East Asia, South & Southeast Asia; note the different axis scales), and none for 2090. We emphasize that the results presented here do not include sea salt and dust derived particulate matter, and are not downscaled using information on the emissions attributable to urban regions. In fact, in Figs. 2 and 3 small areas with typical urban population densities e.g. above 1000 / km^2 are included in same category in with the much larger areas in the 100 to 1000 km^{-2} range. Therefore these results are likely to represent a lower limit of population-weighted $PM_{2.5}$ concentrations, which are consequently closer to the WHO guidelines. In general, relative changes in per-area emissions (Fig. 2) are much larger than relative changes in concentrations (Fig. 3), mainly due to the effect of long-range atmospheric transport of aerosols and precursor gases.

In contrast to the current situation with a steady increase in pollutant concentrations with population density (dark blue in Fig. 3), for 2090 concentrations peak at an intermediate level of population density in most regions (red line: Sub-Saharan Africa, Latin America & Caribbean, Eastern Europe-Russia-Central Asia, Australia & New Zealand, High-Income Europe), reflecting the increased importance of wildfires for the spatial distribution of pollutant concentrations. This change over time is most pronounced for Sub-Saharan Africa, where emissions from wildfires far outweigh anthropogenic $PM_{2.5}$ emissions by 2090 (Fig. 2, red lines).

The effect of the anthropogenic-emissions scenario can be seen by comparing the MFR and CLE scenarios for the case of the high-wildfire emissions scenario (red and green lines in Fig. 3, cf. Table 1). CLE/SSP5/RCP8.5 compared to

MFR/SSP5/RCP8.5 leads to large reductions in concentrations in pollutant concentrations in all regions by 2090, in particular for the most densely populated categories. Compared to this large effect of the anthropogenic emissions scenario, the effect of the wildfire scenario (difference between high and low wildfire-emissions scenario, red and light-blue lines in Fig. 3) is relatively small and only visible in Sub-Saharan Africa, South & South-East Asia and Developing East Asia.

Simulated spatial patterns of $PM_{2.5}$ concentrations for current conditions as well as for the CLE scenario (Fig. 4 a, b) show large parts of central Africa as well as most of South, East and Southeast Asia with concentrations above the WHO air quality guidance value. For MFR (Fig. 4c, d), however, only limited areas in central Africa show levels exceeding 10 $\mu g / m^3$. For the high-wildfire scenario (SSP5/RCP8.5, Fig. 4d), concentrations are higher than for low-wildfire emissions (SSP3/RCP4.5, Fig. 4c), but the areas are much more sparsely populated (see Fig. S4). It appears therefore that under the MFR scenario, annual mean anthropogenic and wildfire-induced concentrations will remain below the WHO air-quality guidance value for most areas of the globe. Even though the previous analysis (Fig. 3) showed wildfire emissions becoming the dominant source for the high-wildfire scenario, it appears the levels of emissions are not high enough to bring concentrations above the annual WHO air-quality value.

Further analysis hereafter focuses on monthly mean $PM_{2.5}$ concentrations, assuming this to be a health-related variable more appropriately reflecting the seasonality of fire emissions. We note that there is currently no guideline for monthly concentrations, but the WHO does provide guidelines for 24-hour means that amount to 25 $\mu g\ m^{-3}$. We here assume that formally declared safe monthly $PM_{2.5}$ concentrations would be somewhere between 10 and 25 $\mu g\ m^{-3}$. When investigating

monthly $PM_{2.5}$ concentrations, the picture changes considerably. For all scenarios, large but sparsely populated regions in central South America, northeastern Siberia and northwestern Canada (cf. Fig. S5) experience monthly pollution levels in excess of 10 µg / m^3 (Fig. 5) and to a lesser extent 25 µg / m^3. This result is largely independent of the anthropogenic-emissions scenario (comparing Fig. 5b with 5c, d). In regions that show large reductions of annual mean pollution levels for MFR, monthly maximum concentrations can still substantially surpass 10 µg / m^3 even under an MFR scenario (Africa, Southeast Asia and, to some extent for SSP5/RCP8.5, south-eastern China), or even 25 µg m^{-3} (Africa, South-East Asia). The wildfire scenario is thus found to be of globally limited, but regionally important significance for air pollution-related health impacts.

4 Discussion

In most regions of the world, decisive and effective reductions of anthropogenic air pollutant emissions will likely be able to limit pollutant levels below the WHO threshold of 10 µg / m^3 annual mean $PM_{2.5}$ concentrations irrespective of the evolution of future wildfire emissions. This is mainly the result of the highly seasonal character of wildfire emissions, as well as a tendency of wildfire sources to be situated in areas of intermediate population density, as opposed to anthropogenic sources that tend to be highest at the highest population densities. We therefore see a shift of the highest pollution levels away from the most densely populated areas, which reduces the impacts of future human exposure to $PM_{2.5}$. However, as the example of the Russian wildfires in 2010 shows (Kaiser et al. 2012), high pollution levels even from single wildfires can persist over many weeks and thus pose a significant health threat over extended lengths of time. On a seasonal basis, we

449 therefore find many regions where pollution levels can reach dangerous levels even
450 for a scenario of aggressive reduction of anthropogenic emissions.
451 Previous simulations with chemistry-climate models using RCP emission
452 projections have already shown a strong future downward trend in East and South
453 Asia, driven by reduced anthropogenic emissions, but no notable trend in Africa
454 (Fiore et al. 2012). Knorr et al. (2016a) have shown a general picture of climate-
455 driven fire emission increases, both for an RCP 4.5 and 8.5 scenario, that may be
456 overridden by demographic changes only in Sub-Saharan Africa. This simulated
457 future decline in Africa is in agreement with observations of currently already
458 declining burned area that has been linked to demographic trends of increasing rural
459 population for the northern part of Sub-Saharan Africa (Andela and van der Werf,
460 2014). In the present study, southern China is identified as a new area of possible high
461 human exposure to wildfire-generated air pollution under a scenario of rapid
462 urbanisation and population decline in rural areas. While forest fires in China may
463 have received comparatively little attention, they can still be substantial, with over
464 670,000 ha area burnt annually between 1950 and 2010 (Shu et al. 2003, Su et al.
465 2015).
466 While any additional emission source of $PM_{2.5}$ poses a health risk (WHO 2006),
467 wildfires are likely to be ignored by air quality policy if they emit considerably less
468 than anthropogenic sources, in particular as their occurrence tends to be sporadic and
469 of short-term nature. One factor is that wildfire emissions are much more difficult to
470 legislate given the difficulties of long-term fire suppression (Donovan and Brown
471 2007). In this study, we find that in large parts of the world, wildfires are the main air
472 pollutant source. While on an annual-mean basis, they are unlikely to lift pollution

levels above the WHO air-quality guidance levels, they can become important sources on a seasonal basis.

In our simulations, air pollutant concentrations follow similar, but more dispersed patterns compared to emissions, with highest levels in densely populated and lowest in sparsely populated areas. In the future, in the case of strong reduction in anthropogenic sources, this pattern is predicted to shift to one where the highest pollution levels are found in regions of intermediate population density for most regions (Sub-Saharan Africa, Latin America & Caribbean, and Eastern Europe-Russia-Central Asia), resembling more the pattern of wildfire emissions. This means that also due to their geographical distribution, wildfires pose a smaller risk to humans than anthropogenic emissions. Nevertheless, in our simulations under strong emission reduction from anthropogenic sources, the future trajectory of wildfire emissions has a discernible impact on air pollution in certain regions (Sub-Saharan Africa, South & Southeast Asia, and Developing East Asia), and is particularly relevant if we consider seasonal maxima in pollution levels. Even though the WHO recommendations are based on annual mean concentrations of $PM_{2.5}$, the WHO also states that health effects persist below these values. Fire emissions typically occur on the timescale of a week up to one or several months – the length of the fire season – and the WHO annual guidelines do not account for such monthly timescales. We hypothesise that, if a guidance level for monthly means were to be established, it would lie somewhere between 10 (annual) and 25 $\mu g / m^3$ (daily WHO air-quality guidance). These levels of $PM_{2.5}$ concentration are indeed frequently exceeded in our simulations even with the extremely low emission levels taken here for the MFR scenario. It also needs to be taken into account that the $PM_{2.5}$ levels that are reported and compared to WHO or other air-quality guidelines usually include some water content, as opposed to the

simulated concentrations of dry aerosol mass, leading to a possible low bias of our simulations of the order of 30 to 50% (Tsyro 2005). Also some emissions and components are not considered in our simulation (e.g. the ash component of fire emissions), or have a very high uncertainty (e.g. secondary aerosol formation associated with burning emissions, but also in general with vegetation emissions).

Significant health impacts are therefore very likely, even if this limit is exceeded only on a seasonal basis. For certain regions, it will be of critical importance whether future air quality policy objectives will converge to the current WHO guidelines, in which case fire management will become increasingly important. If anthropogenic emissions are aggressively curtailed (MFR scenario), wildfires in Sub-Saharan Africa are predicted to decline less than anthropogenic sources, and in parts of Southeast Asia, southern China and central South America climate change may even lead to new areas with wildfire emission levels relevant for air quality and the associated health impacts. In many boreal regions wildfires will also increase to levels where they become pollution sources with relevant health impacts. Because past efforts aimed at a lasting reduction in wildfire activity have largely failed (Donovan et al. 2007, Doerr and Santin 2016), it is questionable whether it is even possible to devise policy measure aimed at bringing down wildfire emissions to avoid adverse health effects.

LPJ-GUESS-SIMFIRE only simulates wildfires. The predictions presented in this study therefore leave out the possibility of significant increases or decreases in deforestation or peat fire sources. Peat fires can be associated with considerable emissions (Page et al. 2002, Kajii et al. 2002), and forest conversion into cropland or pasture is often accompanied by burning (van der Werf et al. 2010). Both are of minor importance for air pollution except for Southeast Asia (see Fig. S1, Table S2), mainly in Indonesia (Field et al. 2009), where they are the dominant pollution source and

523 occur even in more densely populated areas. In other regions, including Russia, peat
524 fires are of minor importance. Whether or not future land-use change will lead to an
525 increase or a decrease in deforestation is unknown. Based on integrated-assessment
526 model realisations of the four RCPs, Hurtt et al. (2011) projected little increase or
527 even a decline in future crop and pasture areas. However, in studies that assessed
528 future land-use change from a broader perspective, a much larger range of crop and
529 pasture changes emerged (Eitelberg et al. 2015, Prestele et al. 2016), which makes the
530 relative change of deforestation vs. wildfires highly uncertain. In the present analysis,
531 declining wildfire emissions are only predicted for Sub-Saharan Africa, where it
532 appears to be related to conversion of savanna to cropland (Andela and van der Werf
533 2014).

534 Apart from the issue of dry vs. wet aerosols and the omission of some difficult to
535 model components, there are additional limitations of this study. We expect that
536 results will be affected by the presence of natural aerosols, such as mineral dust and
537 sea salt, which – depending on location and time of year – could be significant
538 fractions of the $PM_{2.5}$ concentrations (Monks et al. 2009). We do not evaluate
539 changes in natural emissions of mineral dust, sea salt or other naturally occurring
540 emissions other than biomass burning. Also, the anthropogenic emission scenarios do
541 not consider the benefits of climate mitigation scenarios, and are based on rather
542 crude assumptions regarding the development of emission controls beyond 2050, as
543 the original scenarios do not consider developments beyond that year. The scenarios
544 are thus study are only a subset of a large range identified in recent studies
545 (Braspenning-Radu et al. 2016, Rao et al. 2016) and therefore call for a further
546 evaluation of consistency in drivers across anthropogenic emissions, climate, and fire
547 scenarios. The study furthermore only considers climatological monthly emissions

548 during specified time windows, even though wildfire impacts on air quality can have
549 large interannual (Jaffe et al. 2008) and intra-seasonal variations. We also did not
550 account for relevant secondary emission products, such as ozone from wildfires,
551 which can reach policy-relevant levels (Jaffe and Wigder 2012). Other studies on the
552 possible impact of climate change on wildfire-related air pollution hazards have
553 concentrated on changes in meteorological conditions (Jacob and Winner 2009, Tai et
554 al. 2010) instead of emissions. There is also recent progress in the incorporation of
555 injection height (Sofiev et al. 2012) into chemistry-enabled atmospheric general
556 circulation models (Veira et al. 2015),which is not considered.

557 Nevertheless, to our knowledge, this is the first global-scale air quality study to
558 consider changes in both climate and demographic drivers of air pollutant emissions
559 from wildfires. Future work should aim at using general circulation models with
560 realistic plume heights for a series of dedicated present and future time slices at
561 combining observed plume height information, fire radiative energy data (for their
562 finer temporal resolution), satellite-derived burned area (for better spatial coverage),
563 projected emission changes from coupled dynamic vegetation-fire models (as the
564 present study), and improved demographic scenarios accounting for changes in urban
565 population density. Such studies would then also simulate the temporal statistics of
566 pollution events on a daily time scale. Wildfire episodes can elevate $PM_{2.5}$ pollution
567 levels to dangerous levels with serious health impacts (Haikerwal et al. 2015). Such
568 results could then be used, for example, to assess for how many days the WHO 24-
569 hour $PM_{2.5}$ limit of 25 $\mu g/m^3$ from the WHO air quality guidelines (WHO 2006) is
570 exceeded as a result of wildfire emissions.

571 # 5 Summary and conclusions

572 • Globally, wildfire emissions are unlikely to thwart aggressive measures to reduce
573 anthropogenic pollutant emissions enough to stay under the ambitious 10 μg / m^3
574 annual mean limit of the WHO.
575 • In a number of regions, wildfire emissions will remain or could rise above critical
576 thresholds relevant for health policy, in particular when pollution levels during the
577 fire season are considered. So far, there is no generally accepted method for
578 wildfire management that has been shown to lead to lasting reductions in fire
579 activity or emissions.
580 • Demographic changes appear to be the main driver for the expected changes in
581 wildfire emissions in Sub-Saharan Africa. For a scenario of high population
582 growth and slow urbanisation, anthropogenic sources could surpass air pollutant
583 emissions from wildfires in most populated areas. Exposure of humans to $PM_{2.5}$ in
584 Sub-Saharan Africa is expected to drop if measures are put in place to reduce
585 anthropogenic emissions, but wildfires may remain as a health relevant pollution
586 source in a scenario of fast urbanisation and low population growth.

587 ## Acknowledgements

588 This work was supported by EU contracts 265148 (Pan-European Gas-Aerosol-
589 climate interaction Study, PEGASOS) and 603542 (Land-use change: assessing the
590 net climate forcing, and options for climate change mitigation and adaptation,
591 LUC4C) as well as BECC (Biodiversity and Ecosystem services in a Changing
592 Climate) funded by the Swedish Government. The National Center for Atmospheric
593 Research is sponsored by the National Science Foundation.
594 **Author contributions:** WK conceived of the study, carried out the analysis and wrote
595 the first draft of the manuscript. JFL performed the CAM-Chem simulations. All
596 authors contributed to discussions and writing.

References

Ahlström, A., Schurgers, G., Arneth, A., and Smith, B.: Robustness and uncertainty in terrestrial ecosystem carbon response to CMIP5 climate change projections, Env. Res. Lett., 7, 044008, doi: 10.1088/1748-9326/7/4/044008, 2012.

Akagi, S. K., Yokelson, R. J., Wiedinmyer, C., Alvarado, M. J., Reid, J. S., Karl, T., Crounse, J. D., and Wennberg, P. O.: Emission factors for open and domestic biomass burning for use in atmospheric models, Atmos Chem Phys, 11, 4039-4072, 2011.

Amann, M., Bertok, I., Borken-Kleefeld, J., Cofala, J., Heyes, C., Höglund-Isaksson, L., Klimont, Z., Nguyen, B., Posch, M., and Rafaj, P.: Cost-effective control of air quality and greenhouse gases in Europe: Modeling and policy applications, Environmental Modelling & Software, 26, 1489-1501, 2011.

Amatulli, G., Camia, A., and San-Miguel-Ayanz, J.: Estimating future burned areas under changing climate in the EU-Mediterranean countries, Sci. Total Environ., 450-451, 209-222, 2013.

Andela, N. and van der Werf, G. R.: Recent trends in African fires driven by cropland expansion and El Nino to La Nina transition, Nature Climate Change, 4, 791-795, 2014.

Archibald, S., Roy, D. P., van Wilgen, B. W., and Scholes, R. J.: What limits fire? An examination of drivers of burnt area in Southern Africa, Global Change Biol, 15, 613-630, 2009.

Archibald, S., Scholes, R. J., Roy, D. P., Roberts, G., and Boschetti, L.: Southern African fire regimes as revealed by remote sensing, Int J Wildland Fire, 19, 861-878, 2010.

Bistinas, I., Harrison, D. E., Prentice, I. C., and Pereira, J. M. C.: Causal relationships

622 vs. emergent patterns in the global controls of fire frequency, Biogeosci., 11,
623 5087–5101, 2014.
624 Bowman, D. M. J. S., Balch, J. K., Artaxo, P., Bond, W. J., Carlson, J. M., Cochrane,
625 M. A., D'Antonio, C. M., DeFries, R. S., Doyle, J. C., Harrison, S. P., Johnston, F.
626 H., Keeley, J. E., Krawchuk, M. A., Kull, C. A., Marston, J. B., Moritz, M. A.,
627 Prentice, I. C., Roos, C. I., Scott, A. C., Swetnam, T. W., van der Werf, G. R., and
628 Pyne, S. J.: Fire in the Earth System, Science, 324, 481-484, 2009.
629 Braspenning-Radu, O., van der Berg, M., Deetman, S., Klimont, Z., Janssens-
630 Maenhout, G., Muntean, M., Dentener, F. J., and van Vuuren, D. P.: Exploring
631 synergies between climate and air quality policies using long-term global and
632 regional emission scenarios, Atm. Environ., 140, 577-591, 2016.
633 Buitenwerf, R., Bond, W. J., Stevens, N., and Trollope, W. S. W.: Increased tree
634 densities in South African savannas: > 50 years of data suggests CO2 as a driver,
635 Global Change Biol, 18, 675-684, 2012.
636 Doerr, S. H. and Santín, C.: Global trends in wildfire and its impacts: perceptions
637 versus realities in a changing world, Phil. Trans. R. Soc. B, 371, 20150345, 2016.
638 Donohue, R. J., Roderick, M. L., McVicar, T. R., and Farquhar, G. D.: Impact of CO2
639 fertilization on maximum foliage cover across the globe's warm, arid
640 environments, Geophys. Res. Lett., 40, 3031-3035, 2013.
641 Donovan, G. H. and Brown, T. C.: Be careful what you wish for: the legacy of
642 Smokey Bear, Frontiers in Ecology and the Environment, 5, 73-79, 2007.
643 Eitelberg, D. A., Vliet, J., and Verburg, P. H.: A review of global potentially available
644 cropland estimates and their consequences for model-based assessments, Global
645 Change Biology, 21, 1236-1248, 2015.
646 EEA: Air quality in Europe - 2014 report, European Environmental Agency Report

No 5/2014, 80 pp., doi:10.2800/22775, 2014.

Field, D. F., van der Werf, G. R., and Shen, S. S. P.: Human amplification of drought-induced biomass burning in Indonesia since 1960, Nature Geosci., 2, 185-188, 2009.

Fiore, A. M., Naik, V., Spracklen, D. V., Steiner, A., Unger, N., Prather, M., Bergmann, D., Cameron-Smith, P. J., Cionni, I., and Collins, W. J.: Global air quality and climate, Chem. Soc. Rev., 41, 6663-6683, 2012.

Flannigan, M., Logan, K. A., Amiro, B. D., Skinner, W. R., and Stocks, B. J.: Future area burned in Canada, Clim. Change, 72, 1-16, 2005.

Flannigan, M. D., Krawchuk, M. A., de Groot, W. J., Wotton, B. M., and Gowman, L. M.: Implications of changing climate for global wildland fire, Int. J. Wildland Fire, doi: 10.1071/wf08187, 2009. 483-507, 2009.

Giglio, L., Randerson, J. T., and van der Werf, G. R.: Analysis of daily, monthly, and annual burned area using the fourth-generation global fire emissions database (GFED4), J Geophys Res-Biogeo, 118, 317-328, 2013.

Granier, C., Bessagnet, B., Bond, T., D' Angiola, A., van der Gon, H. D., Frost, G. J., Heil, A., Kaiser, J. W., Kinne, S., Klimont, Z., Kloster, S., Lamarque, J. F., Liousse, C., Masui, T., Meleux, F., Mieville, A., Ohara, T., Raut, J.-C., Riahi, K., Schultz, M. G., Smith, S. J., Thompson, A., von Aardenne, J., van der Werf, G. R., and Vuuren, D. P.: Evolution of anthropogenic and biomass burning emissions of air pollutants at global and regional scales during the 1980–2010 period, Clim. Change, 109, 163–190, 2011.

Guyette, R. P., Muzika, R. M., and Dey, D. C.: Dynamics of an anthropogenic fire regime, Ecosystems, 5, 472-486, 2002.

Haikerwal, A., Akram, M., Del Monaco, A., Smith, K., Sim, M. R., Meyer, M.,

672 Tonkin, A. M., Abramson, M. J., and Dennekamp, M.: Impact of fine particulate
673 matter (PM2. 5) exposure during wildfires on cardiovascular health outcomes,
674 Journal of the American Heart Association, 4, e001653, doi:
675 10.1161/JAHA.114.001653, 2015.
676 Hurtt, G. C., Chini, L. P., Frolking, S., Betts, R. A., Feddema, J., Fischer, G., Fisk, J.
677 P., Hibbard, K., Houghton, R. A., Janetos, A., Jones, C. D., Kindermann, G.,
678 Kinoshita, T., Goldewijk, K. K., Riahi, K., Shevliakova, E., Smith, S., Stehfest, E.,
679 Thomson, A., Thornton, P., van Vuuren, D. P., and Wang, Y. P.: Harmonization of
680 land-use scenarios for the period 1500-2100: 600 years of global gridded annual
681 land-use transitions, wood harvest, and resulting secondary lands, Climatic
682 Change, 109, 117-161, 2011.
683 IEA: Energy Technology Perspectives 2012, International Energy Agency, Paris, 690
684 pp., 2012.
685 Jacob, D. J. and Winner, D. A.: Effect of climate change on air quality, Atmos
686 Environ, 43, 51-63, 2009.
687 Jaffe, D., Chand, D., Hafner, W., Westerling, A., and Spracklen, D.: Influence of fires
688 on O3 concentrations in the western US, Environmental science & technology, 42,
689 5885-5891, 2008.
690 Jaffe, D. A. and Wigder, N. L.: Ozone production from wildfires: A critical review,
691 Atmos. Environ., 51, 1-10, 2012.
692 Jiang, L.: Internal consistency of demographic assumptions in the shared
693 socioeconomic pathways, Popul. Environ., 35, 261-285, 2014.
694 Jiang, L. and O'Neill, B. C.: Global urbanization projections for the Shared
695 Socioeconomic Pathways, Global Environmental Change, 2015. 2015.
696 Kaiser, J. W., Heil, A., Andreae, M. O., Benedetti, A., Chubanova, N., Jones, L.,

697 Mocrette, J.-J., Razinger, M., Schultz, M. G., Suttie, M., and van der Werf, G. R.:
698 Biomass burning emissions estimated with a global fire assimilation system based
699 on observed fire radiative power, Biogeosci., 9, 527-554, 10.5194/bg-9-527-2012,
700 2012.
701 Kajii, Y., Kato, S., Streets, D. G., Tsai, N. Y., Shvidenko, A., Nilsson, S., McCallum,
702 I., Minko, N. P., Abushenko, N., and Altyntsev, D.: Boreal forest fires in Siberia in
703 1998: Estimation of area burned and emissions of pollutants by advanced very high
704 resolution radiometer satellite data, Journal of Geophysical Research:
705 Atmospheres, 107, 2002.
706 Kelley, D. I. and Harrison, S. P.: Enhanced Australian carbon sink despite increased
707 wildfire during the 21st century, Environ. Res. Lett., 9, 104015, doi: 10.1088/1748-
708 9326/9/10/104015, 2014.
709 Klein Goldewijk, K., Beusen, A., and Janssen, P.: Long-term dynamic modeling of
710 global population and built-up area in a spatially explicit way: HYDE 3.1,
711 Holocene, 20, 565-573, 2010.
712 Klimont, Z., Smith, S. J., and Cofala, J.: The last decade of global anthropogenic
713 sulfur dioxid: 2000-2011 emissions, Environ. Res. Lett., 8, 014003, 2013.
714 Kloster, S., Mahowald, N. M., Randerson, J. T., Thornton, P. E., Hoffman, F. M.,
715 Levis, S., Lawrence, P. J., Feddema, J. J., Oleson, K. W., and Lawrence, D. M.:
716 Fire dynamics during the 20th century simulated by the Community Land Model,
717 Biogeosci., 7, 1877-1902, 2010.
718 Knorr, W., Lehsten, V., and Arneth, A.: Determinants and predictability of global
719 wildfire emissions, Atm. Chem. Phys., 12, 6845–6861, 2012.
720 Knorr, W., Kaminski, T., Arneth, A., and Weber, U.: Impact of human population
721 density on fire frequency at the global scale, Biogeosci., 11, 1085-1102, 2014.

722 Knorr, W., Dentener, F., Hantson, S., Jiang, L., Klimont, Z., and Arneth, A.: Air
723 quality impacts of European wildfire emissions in a changing climate, Atmos.
724 Chem. Phys, 16, 5685-5703, 2016a.
725 Knorr, W., Jiang, L., and Arneth, A.: Climate, CO_2, and demographic impacts on
726 global wildfire emissions, Biogeosci., 13, 267-282, 2016b.
727 Knorr, W., Arneth, A., and Jiang, L.: Demographic controls of future global fire risk,
728 Nature Climate Change, doi: 10.1038/NCLIMATE2999, 2016c.
729 Krawchuk, M. A., Moritz, M. A., Parisien, M. A., Van Dorn, J., and Hayhoe, K.:
730 Global Pyrogeography: the Current and Future Distribution of Wildfire, Plos One,
731 4, e5102, doi: 10.1371/journal.pone.0005102, 2009.
732 Lamarque, J.-F., Emmons, L., Hess, P., Kinnison, D. E., Tilmes, S., Vitt, F., Heald,
733 C., Holland, E. A., Lauritzen, P., and Neu, J.: CAM-chem: Description and
734 evaluation of interactive atmospheric chemistry in the Community Earth System
735 Model, Geoscientific Model Development, 5, 369, 2012.
736 Langmann, B., Duncan, B., Textor, C., Trentmann, J., and van der Werf, G. R.:
737 Vegetation fire emissions and their impact on air pollution and climate, Atmos
738 Environ, 43, 107-116, 2009.
739 Lee, K. H., Kim, J. E., Kim, Y. J., Kim, J., and von Hoyningen-Huene, W.: Impact of
740 the smoke aerosol from Russian forest fires on the atmospheric environment over
741 Korea during May 2003, Atmos. Environ., 39, 85-99, 2005.
742 Lehsten, V., Harmand, P., Palumbo, I., and Arneth, A.: Modelling burned area in
743 Africa, Biogeosciences, 7, 3199-3214, 2010.
744 Marlier, M. E., DeFries, R. S., Kim, P. S., Gaveau, D. L. A., Koplitz, S. N., Jacob, D.
745 J., Mickley, L. J., Margono, B. A., and Myers, S. S.: Regional air quality impacts
746 of future fire emissions in Sumatra and Kalimantan, Environ. Res. Lett., 10,

747 054010, doi:10.1088/1748-9326/10/5/054010, 2015.
748 Marlon, J. R., Bartlein, P. J., Carcaillet, C., Gavin, D. G., Harrison, S. P., Higuera, P.
749 E., Joos, F., Power, M. J., and Prentice, I. C.: Climate and human influences on
750 global biomass burning over the past two millennia, Nature Geosci., 1, 697-702,
751 2008.
752 Monks, P. S., Granier, C., Fuzzi, S., Stohl, A., Williams, M., Akimoto, H., Amann,
753 M., Baklanov, A., Baltensperger, U., and Bey, I.: Atmospheric composition
754 change–global and regional air quality, Atmos Environ, 43, 5268-5350, 2009.
755 Page, S. E., Siegert, F., Rieley, J., Boehm, H.-D., Jayak, A., and Limink, S.: The
756 amount of carbon released from peat and forest fires in Indonesia during 1997,
757 Nature, 420, 61-65, 2002.
758 Prestele, R., Alexander, P., Rounsevell, M. D. A., Arneth, A., Calvin, K., Doelman, J.,
759 Eitelberg, D. A., Engström, K., Fujimori, S., and Hasegawa, T.: Hotspots of
760 uncertainty in land-use and land-cover change projections: a global-scale model
761 comparison, Global Change Biology, 2016. 2016.
762 Randerson, J., Chen, Y., van der Werf, G. R., Rogers, B. M., and Morton, D. C.:
763 Global burned area and biomass burning emissions from small fires, J. Geophys.
764 Res., 117, G04012, 2012.
765 Rao, S., Klimont, Z., Leitao, J., Riahi, K., van Dingenen, R., Reis, L. A., Calvin, K.,
766 Dentener, F., Drouet, L., and Fujimori, S.: A multi-model assessment of the co-
767 benefits of climate mitigation for global air quality, Environmental Research
768 Letters, 11, 124013, 2016.
769 Shindell, D. T., J.-F. Lamarque, M. Schulz, M. Flanner, C. Jiao, M. Chin, P. J. Young,
770 Y. Lee, G. Milly, G. Faluvegi, Y. Balkanski, W. J. Collins, A. J. Conley, S.
771 Dalsoren, R. Easter, S. J. Ghan, L. Horowitz, X. Liu, G. Myhre, T. Nagashima, V.

772 Naik, L. Rotstayn, S. Rumbold, R. Skeie, K. Sudo, S. Szopa, T. Takemura, J.-H.
773 Yoon, Radiative forcing in the ACCMIP historical and future climate simulations,
774 Atmos. Chem. Phys., 13, 2939-2974, doi:10.5194/acp-13-2939-2013, 2013.
775 Silva, R. A., J. J. West, Y. Zhang, S. C. Anenberg, J.-F. Lamarque, D. T. Shindell, W.
776 J. Collins, S. B. Dalsøren, G. Faluvegi, L. W. Horowitz, T. Nagashima, V. Naik, S.
777 Rumbold, R. Skeie, K. Sudo, T. Takemura, D. Bergmann, P. Cameron-Smith, I.
778 Cionni, R. M. Doherty, V. Eyring, B. Joesse, I. A. MacKenzie, D. Plummer, M.
779 Righi, D. S. Stevenson, S. Strode, S. Szopa, G. Zeng, Global premature mortality
780 due to anthropogenic outdoor air pollution and the contribution of past climate
781 change. Environ. Res. Lett., 8, doi:10.1088/1748-9326/8/3/034005, 2013.
782 Silva, R. A., J. J. West, J.-F. Lamarque, D. T. Shindell, W. J. Collins, S. Dalsoren, G.
783 Faluvegi, G. Folberth, L. W. Horowitz, T. Nagashima, V. Naik, S. T. Rumbold, K.
784 Sudo, T. Takemura, D. Bergmann, P. Cameron-Smith, I. Cionni, R. M. Doherty, V.
785 Eyring, B. Josse, I. A. MacKenzie, D. Plummer, M. Righi, D. S. Stevenson, S.
786 Strode, S. Szopa, and G. Zeng, The effect of future ambient air pollution on human
787 premature mortality to 2100 using output from the ACCMIP model ensemble.
788 Atmos. Chem. Phys., 16, 9847-9862, doi:10.5194/acp-16-9847-2016, 2016.
789 Shu, L., Tian X., and Wang, M.: A study on forest fire occurrence in China. XII
790 World Forestry Congress, Québec City, Canada, 21–28 September,
791 http://www.fao.org/docrep/ARTICLE/WFC/XII/0278-B1.HTM, 2003.
792 Smith, B., Prentice, C., and Sykes, M.: Representation of vegetation dynamics in
793 modelling of terrestrial ecosystems: comparing two contrasting approaches within
794 European climate space, Global Ecol Biogeogr, 10, 621-637, 2001.
795 Sofiev, M., Ermakova, T., and Vankevich, R.: Evaluation of the smoke-injection
796 height from wild-land fires using remote-sensing data, Atmos Chem Phys, 12,

797 1995-2006, 2012.
798 Spracklen, D. V., Mickley, L. J., Logan, J. A., Hudman, R. C., Yevich, R., Flannigan,
799 M. D., and Westerling, A. L.: Impacts of climate change from 2000 to 2050 on
800 wildfire activity and carbonaceous aerosol concentrations in the western United
801 States, Journal of Geophysical Research: Atmospheres, 114, 2009.
802 Stohl, A., Aamaas, B., Amann, M., Baker, L., Bellouin, N., Berntsen, T., Boucher, O.,
803 Cherian, R., Collins, W., and Daskalakis, N.: Evaluating the climate and air quality
804 impacts of short-lived pollutants, Atmos Chem Phys, 15, 10529-10566, 2015.
805 Su, L., He Y. and Chen, S.: Temporal and spatial characteristics and risk analysis of
806 forest fires in China from 1950 to 2010.,Scientia Silvae Sinicae 51, 88-96, 2015 (in
807 Chinese with English abstract and figure captions).
808 Syphard, A. D., Radeloff, V. C., Keeley, J. E., Hawbaker, T. J., Clayton, M. K.,
809 Stewart, S. I., and Hammer, R. B.: Human influence on California fire regimes,
810 Ecological Applications, 17, 1388-1402, 2007.
811 Tai, A. P. K., Mickley, L. J., and Jacob, D. J.: Correlations between fine particulate
812 matter (PM 2.5) and meteorological variables in the United States: Implications for
813 the sensitivity of PM 2.5 to climate change, Atmos Environ, 44, 3976-3984, 2010.
814 Taylor, K. E., Stouffer, R. J., and Meehl, G. A.: An overview of CMIP5 and the
815 experiment design, Bull. Am. Meteorol. Soc., 93, 485-498, 2012.
816 Tilmes, S. , J.-F. Lamarque, L. K. Emmons, D. E. Kinnison, D. Marsh, R. R. Garcia,
817 A. K. Smith, R. R. Neely, A. Conley, F. Vitt, M. ValMartin, H. Tanimoto, I.
818 Simpson, D. R. Blake and N. Blake. Representation of the Community Earth
819 System Model (CESM1) CAM4-chem within the Chemistry-Climate Model
820 Initiative (CCMI). Geosci. Model Dev., 9, 1853-1890, doi:10.5194/gmd-9-1853-
821 2016, 2016.

822 Tsyro, S.: To what extent can aerosol water explain the discrepancy between model
823 calculated and gravimetric PM 10 and PM 2.5?, Atmos Chem Phys, 5, 515-532,
824 2005.
825 van der Werf, G. R., Randerson, J. T., Giglio, L., Collatz, G. J., Mu, M., Kasibhatla,
826 P. S., Morton, D. C., Defries, R. S., Jin, Y., and van Leeuwen, T. T.: Global fire
827 emissions and the contribution of deforestation, savanna, forest, agricultural, and
828 peat fires (1997-2009), Atmos. Chem. Phys., 10, 11707-11735, 2010.
829 van der Werf, G. R., Peters, W., van Leeuwen, T. T., and Giglio, L.: What could have
830 caused pre-industrial biomass burning emissions to exceed current rates?, Clim.
831 Past, 9, 289-306, 2013.
832 van Vuuren, A. J., Edmonds, J., Kainuma, M., Riahi, K., Thomson, A., Hibbard, K.,
833 Hurtt, G. C., Kram, T., Krey, V., Lamarque, J. F., Masui, T., Meinshausen, M.,
834 Naicenovic, N., Smith, S. J., and Rose, S. K.: The representative concentration
835 pathways: an overview, Clim. Change, 109, 5-31, 2011.
836 Veira, A., Kloster, S., Wilkenskjeld, S., and Remy, S.: Fire emission heights in the
837 climate system–Part 1: Global plume height patterns simulated by ECHAM6-
838 HAM2, Atmos Chem Phys, 15, 7155-7171, 2015.
839 Wang, Z., Chappellaz, J., Park, K., and Mak, J. E.: Large variations in Southern
840 Hemisphere biomass burning during the last 650 years, Science, 330, 1663-1666,
841 2010.
842 West, J. J., S. J. Smith, R.l A. Silva, V. Naik, Y. Zhang, Z. Adelman, M. M. Fry, S.
843 Anenberg, L. W. Horowitz, J.-F. Lamarque, Co-benefits of Global Greenhouse Gas
844 Mitigation for Future Air Quality and Human Health, Nature Climate Change, 3,
845 885-889, doi:10.1038/nclimate2009, 2013.
846 WHO: Air quality guidelines for particulate matter, ozone, nitrogen dioxide and sulfur

847 dioxide, Global update 2005, Summary of risk assessment, World Health
848 Organization, 2006.
849 Yue, X., Mickley, L. J., Logan, J. A., and Kaplan, J. O.: Ensemble projections of
850 wildfire activity and carbonaceous aerosol concentrations over the western United
851 States in the mid-21st century, Atmos Environ, 77, 767-780, 2013.
852 Yue, X., Mickley, L., Logan, J., Hudman, R., Martin, M. V., and Yantosca, R.: Impact
853 of 2050 climate change on North American wildfire: consequences for ozone air
854 quality, Atmos Chem Phys, 15, 10033-10055, 2015.
855

Tables

Table 1: Scenarios and scenario differences considered in the analysis

Case	CAM-Chem	Anthropogenic emissions	Wildfire scenario
0	x	Current	Current
1	x	MFR (lowest)	SSP3/RCP4.5 (lowest)
2	x	MFR (lowest)	SSP5/RCP8.5 (highest)
3	x	CLE (highest)	SSP5/RCP8.5 (highest)
4		CLE (highest)	SSP3/RCP4.5 (lowest)
		Assessment of	
2 - 1		Impact of wildfire scenario on $PM_{2.5}$ emissions	
3 - 2		Impact of air quality policy scenario on $PM_{2.5}$ emissions	

Figures

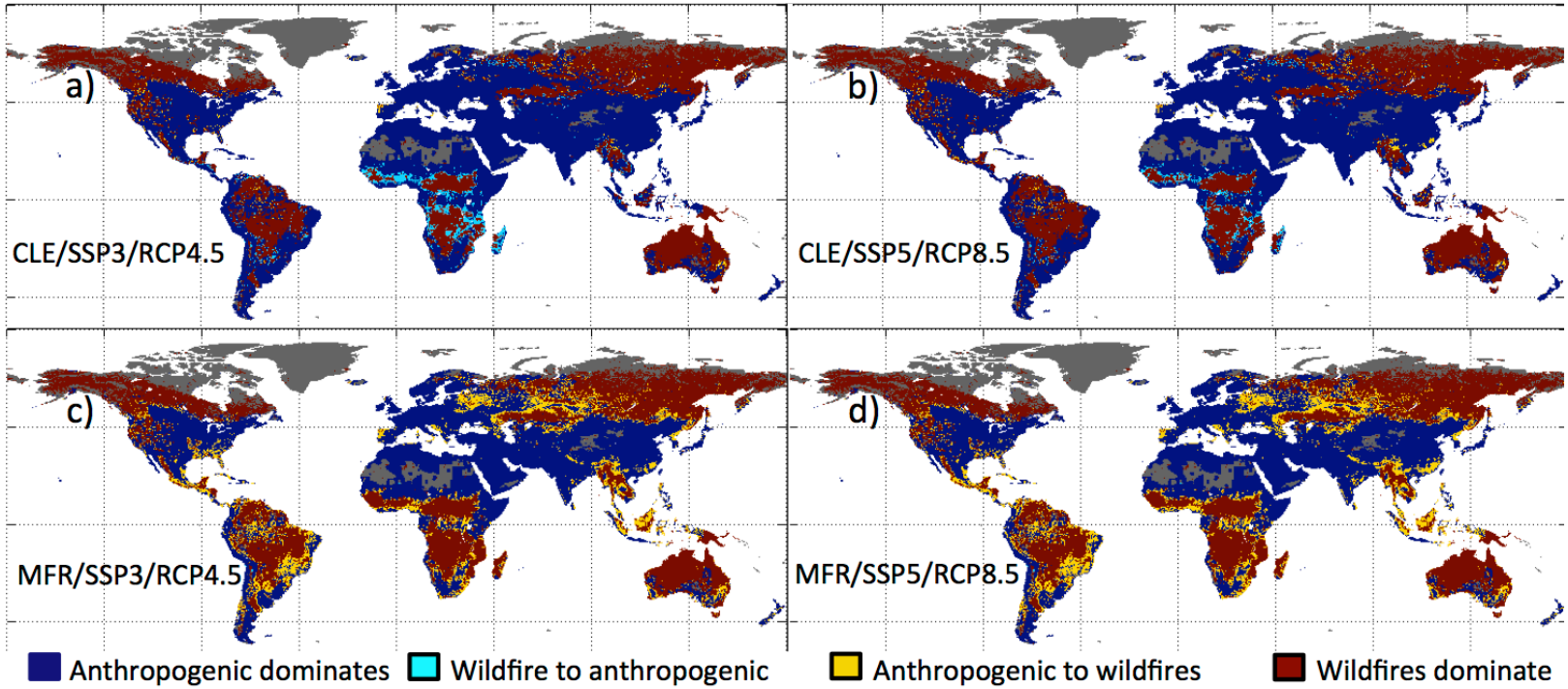

Figure 1: Dominant $PM_{2.5}$ source between anthropogenic and wildfire emissions current and by 2090. Either source dominates if larger than the other. Cases are: dominance for both periods, or transition of dominance from the one to the other, or zero emissions in at least one period (grey areas). a, b) CLE anthropogenic emission scenario (continuing high air pollutant emissions); c, d) MFR anthropogenic scenario (maximum feasible reduction); a, c) SSP3/RCP4.5 wildfire scenario (lowest future emissions); b, d) SSP5/RCP8.5 wildfire scenario (highest future emissions).

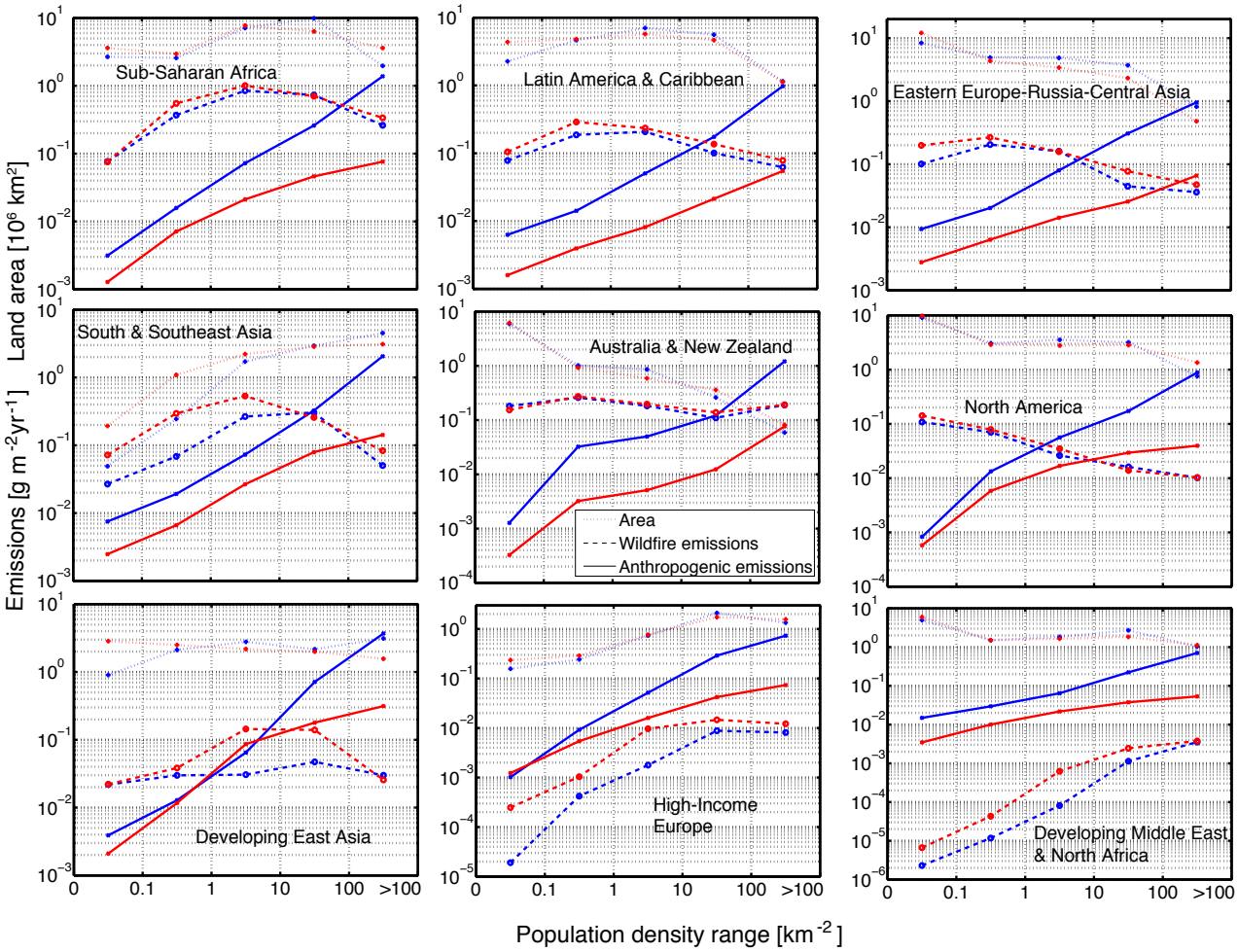

866
867 *Figure 2: Predicted per-area annual $PM_{2.5}$ emissions against ranges of population density for wildfires*
868 *and anthropogenic sources, present (blue) and for 2090 (red) for SSP5/RCP8.5 wildfire scenario*
869 *(highest global emissions) and MFR anthropogenic emissions scenario (maximum-feasible reduction)*
870 *for nine world regions. Also shown are changes in area extent of the population-density categories*
871

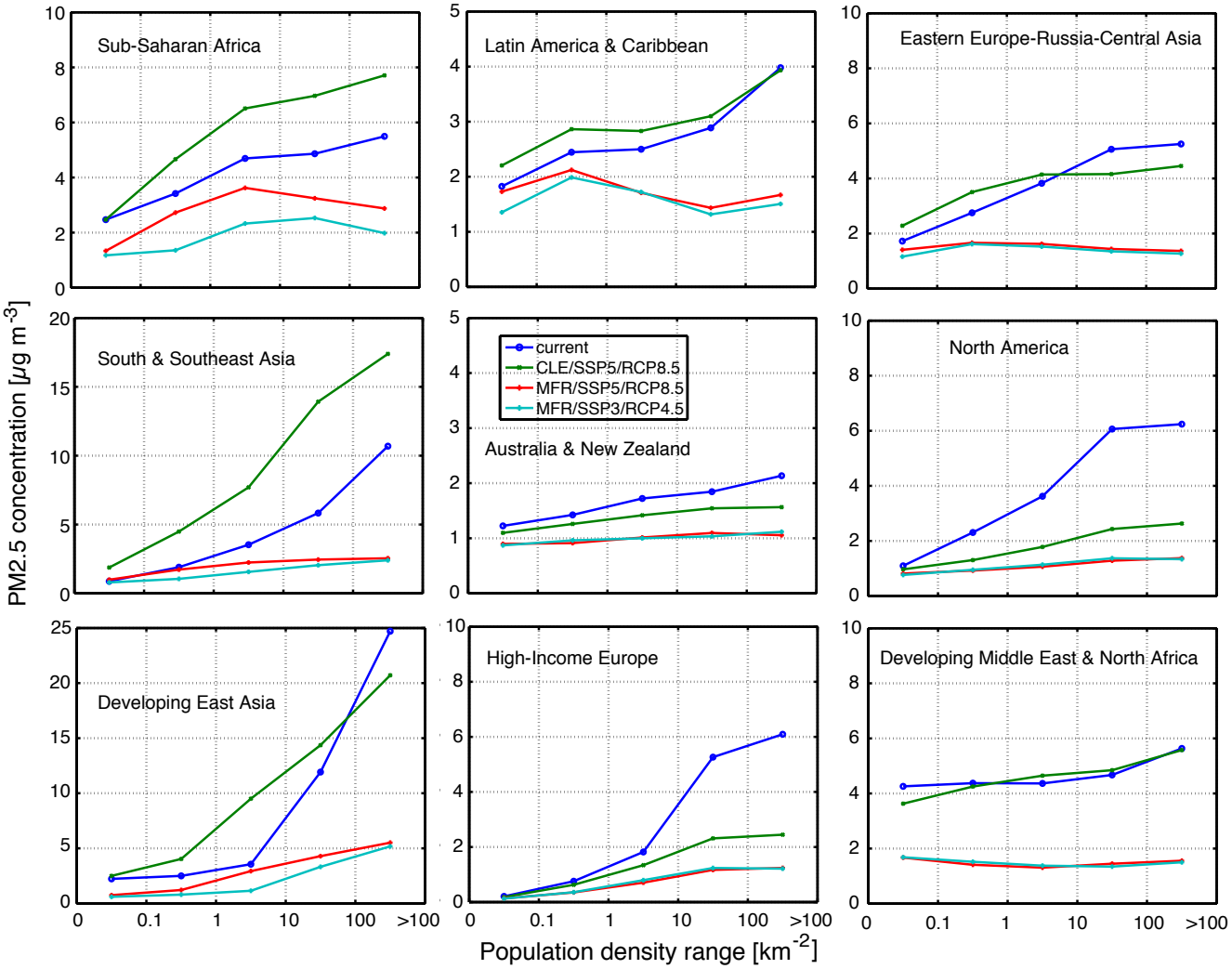

872

873 *Figure 3: Predicted annual PM2.5 concentrations against ranges of population density (excluding*

874 *mineral dust and sea salt) for current conditions and three scenarios for 2090.*

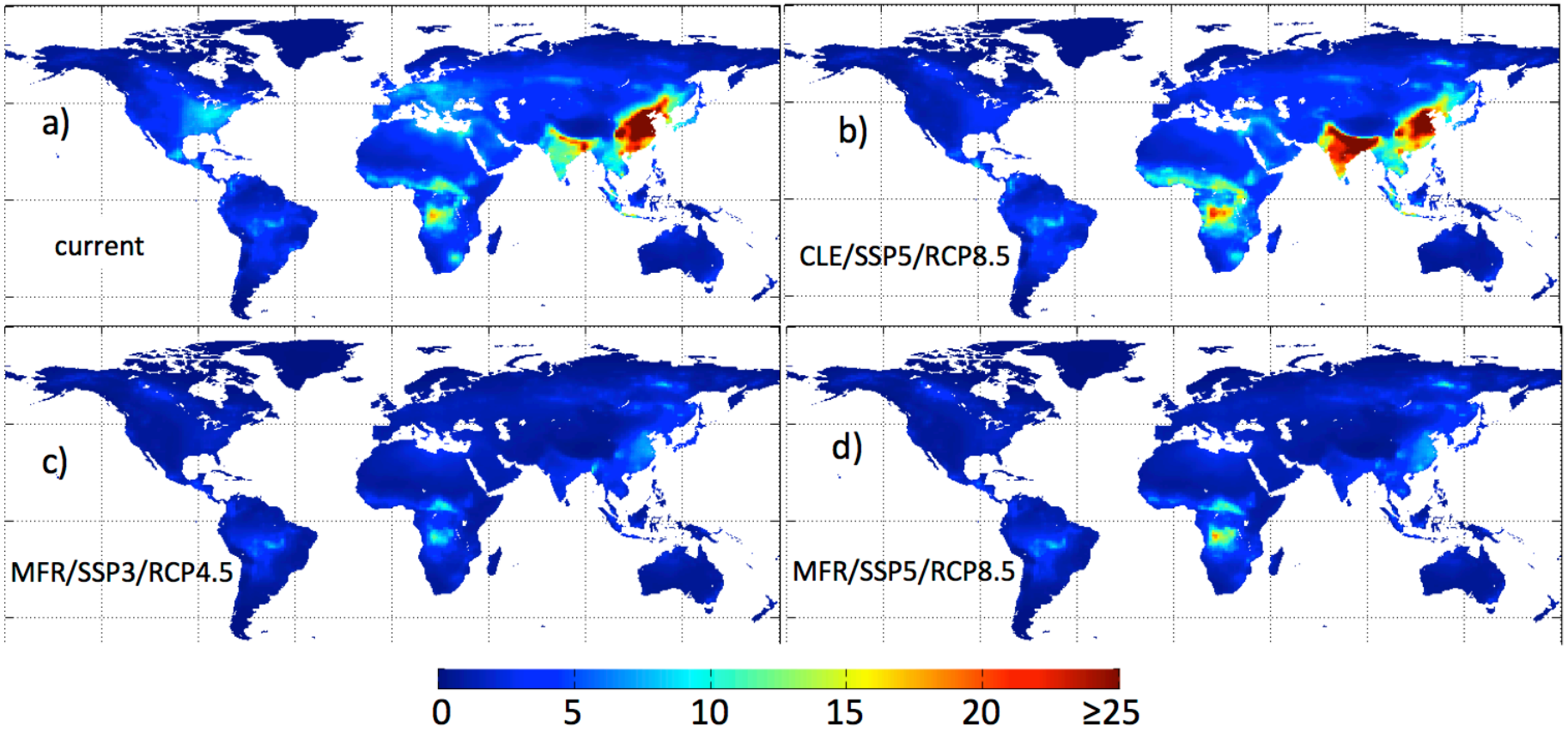

875

876 *Figure 4: Simulated annual-mean anthropogenic and wildfire PM2.5 concentration in µg/m^3. a) current, b) 2090 CLE/SSP5/RCP8.5, c) 2090*

877 *MFR/SSP3/RCP4.5, d) 2090 MFR/SSP5/RCP8.5.*

878

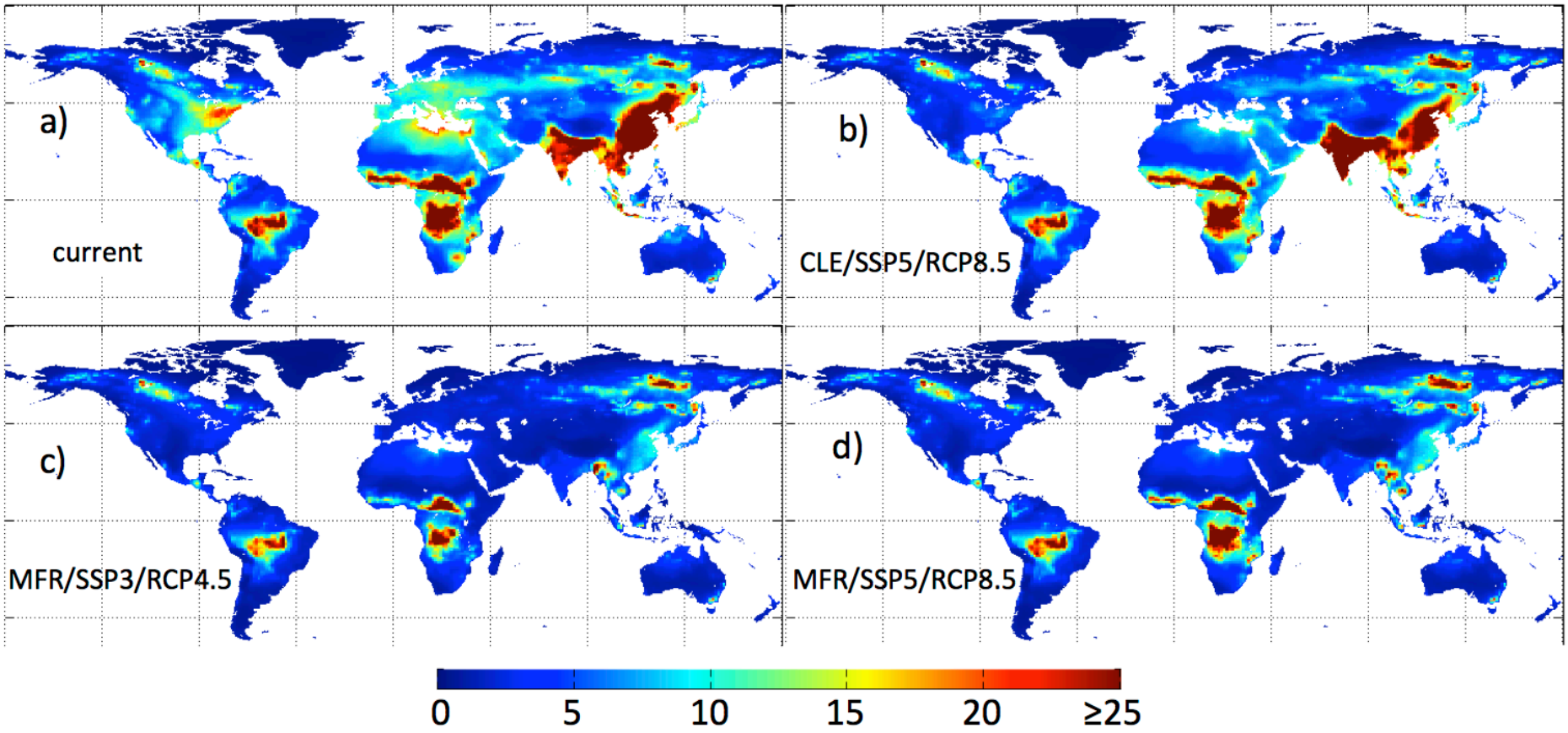

Figure 5: Simulated PM2.5 concentration (excluding mineral dust or sea salt) in µg/m^3 for the month with highest concentration at each grid point. a) current, b) 2090 CLE/SSP5/RCP8.5, c) 2090 MFR/SSP3/RCP4.5, d) 2090 MFR/SSP5/RCP8.5.